JCTC Journal of Chemical Theory and Computation

Article

pubs.acs.org/JCTC

Frozen-Density Embedding Potentials and Chiroptical Properties

T. Daniel Crawford,*[,†] Ashutosh Kumar,[†] Kevin P. Hannon,[†] Sebastian Höfener,[‡] and Lucas Visscher[¶]

[†]Department of Chemistry, Virginia Tech, Blacksburg, Virginia 24061, United States

[‡]Institut für Physikalische Chemie, Karlsruher Institut für Technologie, D-76131 Karlsruhe, Germany

[¶]Amsterdam Center for Multiscale Modeling, VU University Amsterdam, De Boelelaan 1083, 1081 HV Amsterdam, The Netherlands

Supporting Information

ABSTRACT: The efficacy of the frozen density embedding (FDE) approach to the simulation of solvent effects is examined for two key chiroptical properties—specific rotation and circular dichroism spectra. In particular, we have investigated the performance of a wave function-theory-in-density-functional-theory (WFT-in-DFT) FDE approach for computing such properties for the small, rigid chiral compound (*P*)-dimethylallene interacting with up to three water molecules. Although the solvent potential is obtained through DFT, the optical response is computed using coupled cluster linear response theory for mixed electric and magnetic field perturbations. We find that the FDE potential generally yields too small a shift from the isolated molecule as compared to that introduced by the explicit solvent. In one case, the FDE potential fails to reproduce a change in sign of the ORD in which the solute interacts with two solvent molecules. The source of these errors is due primarily to the lack of solvent response to the external field and is analyzed in terms of solvent−solute charge transfer excitations.

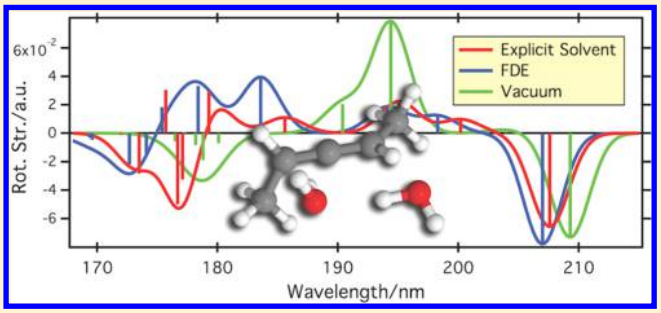

1. INTRODUCTION

Theoretical descriptions of the optical properties of chiral molecules have matured substantially in the last two decades, and numerous studies have demonstrated the requirements for a physically complete and reliable model of these remarkably sensitive properties.[1−5] Careful consideration of numerous factors, including electron correlation, basis-set completeness, gauge representation, zero-point vibrational motion, temperature, conformational flexibility, and so forth, have aided the development of advanced quantum chemical calculations[3,4,6−48] that often yield excellent comparisons with corresponding gas-phase experimental data. Unfortunately, nearly all measurements of molecular chiroptical response—optical rotations (refraction), circular dichroism (absorption), vibrational Raman optical activity (scattering), circularly polarized luminesence (emission), and more—are carried out in *liquid* phases, either in the neat state or in solvent.[30] Thus, equally careful consideration of robust models of solvation is needed for theory to provide accurate predictions of such properties that will be of use in the determination of absolute stereochemical configurations of chiral isolates.[49]

A number of studies have examined the efficacy of both implicit and explicit solvent models for calculating chiral spectra in solution. In 2002, Mennucci and co-workers[50] combined density functional theory (DFT) calculations of specific rotations of methyloxirane with the polarizable continuum model (PCM) for computing the specific rotations of a set of seven chiral compounds. They found that, although the model performed well for solvents such as cyclohexane, acetone, methanol, and acetonitrile, the lack of nonelectrostatic solute−solvent interactions yielded poor agreement with experimental data for carbon tetrachloride, benzene, and chloroform. Similarly, Pecul et al. reported in 2005[51] analogous DFT-based PCM studies of electronic circular dichroism and found that, for certain valence-only transitions, the method provides useful results. However, for more diffuse states and/or systems exhibiting molecule-specific solute−solvent interactions, such as hydrogen bonding or vibronic effects, the performance of the DFT+PCM approach is unreliable.

In 2006 and 2007, Beratan and co-workers examined dynamic solvent effects by combining continuum and molecular dynamics (MD) simulations of methyloxirane in clusters of water[52] and benzene,[53] obtaining DFT-specific rotations as averages over snapshots taken along the MD trajectories. Although they obtained qualitative agreement with experimental data in both cases and found that, although the chiroptical response of the solute molecule was dominant in water, the solvent cavity of benzene contributed at least as much to the total rotation. More recently, Barone and co-workers[54] reported large-scale DFT-based MD simulations of methyloxirane in water that reproduces qualitatively the experimental optical rotatory dispersion curve in water. However, given that DFT has been shown to provide fortuitous agreement with gas-phase experimental data in the case of

Received: September 3, 2015
Published: October 12, 2015

DOI: 10.1021/acs.jctc.5b00845
J. Chem. Theory Comput. 2015, 11, 5305−5315

methyloxirane, the reliability and general applicability of these approaches is uncertain.

The combination of coupled cluster (CC) methods with solvent models for the prediction of chiroptical properties has been somewhat rarer, in part due to the greater computational expense of such high-accuracy quantum chemical models. Kongsted et al.[55,56] published extensive CC analyses for the optical rotation of (*S*)-methyloxirane under solvated conditions, simulated using a continuum dielectric medium surrounding a spherical solute cavity.[55] Despite the inclusion of very high levels of electron correlation (including estimates of connected triple excitations[57,58]), this approach failed to reproduce experimental trends, yielding specific rotations at 355 nm with the wrong sign as compared to measurements in cyclohexane. Caricato[59] reported the first implementation of the CC linear-response approach in conjunction with PCM for polarizabilities and specific rotations and found substantial shifts between gas- and solvent-phase (PCM) results at the sodium D-line. Although these shifts provided at least qualitative agreement with the experimental data for two of the three systems studied, PCM was unable to overcome the incorrect sign for the third.

The focus of the present work is an alternative approach to the inclusion of solvent effects in advanced quantum chemical calculations that is intermediate between the explicit and implicit models described above: frozen-density embedding (FDE) potentials. The FDE idea was first put forward by Wesolowski and Warshel[60,61] in 1993 based on a DFT-in-DFT embedding concept. Carter and co-workers[62,63] later extended the FDE idea to a WFT-in-DFT approach in which the system of interest is described by a wave function-based model while the environment is modeled by DFT, and more recently, Neugebauer[64] has considered the particular problem of computing response properties using FDE potentials. In the FDE concept, the effect of the solvent is approximated by a simple local potential that can be computed using a relatively low level of theory, such as DFT, with explicit inclusion of both the solute and solvent molecules. The resulting potential is then added to the Hamiltonian of a calculation in which the solute is described at a higher level of theory, such as CC, thus providing a significant improvement in comptuational efficiency for the description of the complex solute−solvent interactions.

We describe the first application of the WFT-in-DFT approach toward the computation of electronic chiroptical properties, namely, specific rotations and electronic circular dichroism spectra. We take as our test case the problematic (*P*)-dimethylallene molecule, a rigid structure that displays axial chirality. A previous study[38] reported a surprisingly large difference in the liquid- and gas-phase experimental optical rotations for (*P*)-dimethylallene, an effect not explained by simple structural changes as modeled by Monte Carlo simulations. To examine the efficacy of the FDE approach, we examine a series of "micro-solvated" clusters in which (*P*)-dimethylallene interacts with up to three water molecules. DFT is used to compute the one-electron potential associated with the solvent molecules, and this potential is subsequently deployed within a CC linear-response computation of the corresponding chiroptical response.

2. THEORETICAL BACKGROUND

The rotation of plane-polarized light by a chiral molecule is related to the Rosenfeld optical activity tensor[1,65]

$$\mathbf{G}'(\omega) = -\frac{2\omega}{\hbar}\sum_{j\neq 0}\frac{\mathrm{Im}(\langle\psi_0|\boldsymbol{\mu}|\psi_j\rangle\langle\psi_j|\mathbf{m}|\psi_0\rangle)}{\omega_{j0}^2-\omega^2} \tag{1}$$

where $\boldsymbol{\mu}$ and $\mathbf{m}$ are the electric- and magnetic-dipole operators, respectively, and ω is the frequency of the light. The summation in eq 1 runs over the excited electronic (unperturbed) wave functions ψ_j, each associated with an excitation frequency ω_{j0}. The specific rotation is computed using the trace of $\mathbf{G}'$[3]

$$[\alpha]_\omega = \frac{(72.0\times 10^6)\hbar^2 N_A\omega}{c^2 m_e^2 M}\times\left[\frac{1}{3}\mathrm{Tr}(\mathbf{G}')\right] \tag{2}$$

where $\mathbf{G}'$ and ω are given in atomic units, N_A is Avogadro's number, c is the speed of light (m/s), m_e is the electron rest mass (kg), and M is the molecular mass (amu).

The impact of solvent−solute interactions on the calculation of the Rosenfeld tensor may be modeled using a WFT-in-DFT FDE approach in which the energy functional of a set of N interacting subsystems is given by

$$\begin{aligned}E[\rho_1,\ldots,\rho_N] &= \int\rho_{\mathrm{tot}}(\mathbf{r})\left(\sum_{i=1}^{N}v_i^{\mathrm{nuc}}(\mathbf{r})\right)\mathrm{d}\mathbf{r}\\ &+\frac{1}{2}\int\frac{\rho_{\mathrm{tot}}(\mathbf{r})\rho_{\mathrm{tot}}(\mathbf{r}')}{|\mathbf{r}-\mathbf{r}'|}\,\mathrm{d}\mathbf{r}\,\mathrm{d}\mathbf{r}'+\sum_{i=1}^{N}E_{\mathrm{xc}}[\rho_i]\\ &+E_{\mathrm{xc}}^{\mathrm{nadd}}[\rho_1,\ldots,\rho_N]+\sum_{i=1}^{N}T_s[\rho_i]+E_{\mathrm{kin}}^{\mathrm{nadd}}[\rho_1,\ldots,\rho_N]\end{aligned} \tag{3}$$

where the total electron density of the complete system, ρ_{tot} is the sum of the densities of the subsystems, the electrostatic potential of the ith subsystem is given by v_i^{nuc}, E_{xc} is the exchange-correlation functional, and the nonadditive kinetic-energy functional,[66] T_s^{nadd}, is given by

$$E_{\mathrm{kin}}^{\mathrm{nadd}}[\rho_1,\ldots,\rho_N] = T_s[\rho_{\mathrm{tot}}]-\sum_{i=1}^{N}T_s[\rho_i] \tag{4}$$

with a similar expression for the nonadditive exchange-correlation contribution. Minimization of the total energy functional with respect to the electron density of each subsystem—while keeping the density of the rest of the subsystems frozen—leads to a set of Kohn−Sham-like equations for each system, which are solved iteratively until all subsystem densities are converged. The desired embedding potential for the ith subsystem is obtained as

$$\begin{aligned}v_{\mathrm{emb}}^{(i)}[\rho_1,\ldots,\rho_N] &= \sum_{j\neq i}v_j^{\mathrm{nuc}}(\mathbf{r})+\sum_{j\neq i}\int\frac{\rho_i(\mathbf{r}')}{|\mathbf{r}-\mathbf{r}'|}\,\mathrm{d}\mathbf{r}'+\\ &\left.\frac{\delta E_{\mathrm{xc}}[\rho]}{\delta\rho}\right|_{\rho=\rho_{\mathrm{tot}}(\mathbf{r})}-\left.\frac{\delta E_{\mathrm{xc}}[\rho]}{\delta\rho}\right|_{\rho=\rho_i(\mathbf{r})}+\frac{\delta T_s^{\mathrm{nadd}}[\rho_1,\ldots,\rho_N]}{\delta\rho_i(\mathbf{r})}\end{aligned} \tag{5}$$

This potential may be subsequently transferred to a coupled cluster linear response computation to simulate the effect of the environment on the properties computed for the subsystem in question—in the present work, the solute molecule of interest.

DOI: 10.1021/acs.jctc.5b00845
J. Chem. Theory Comput. 2015, 11, 5305−5315

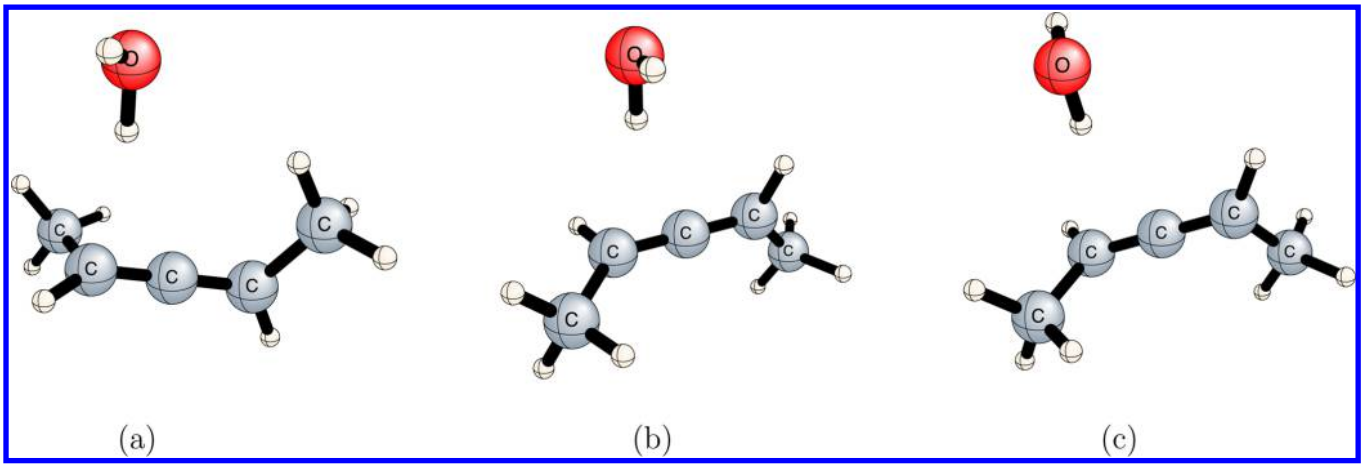

Figure 1. Test configurations of (*P*)-dimethylallene interacting with one water molecule, as optimized at the B3LYP/aug-cc-pVDZ level of theory.

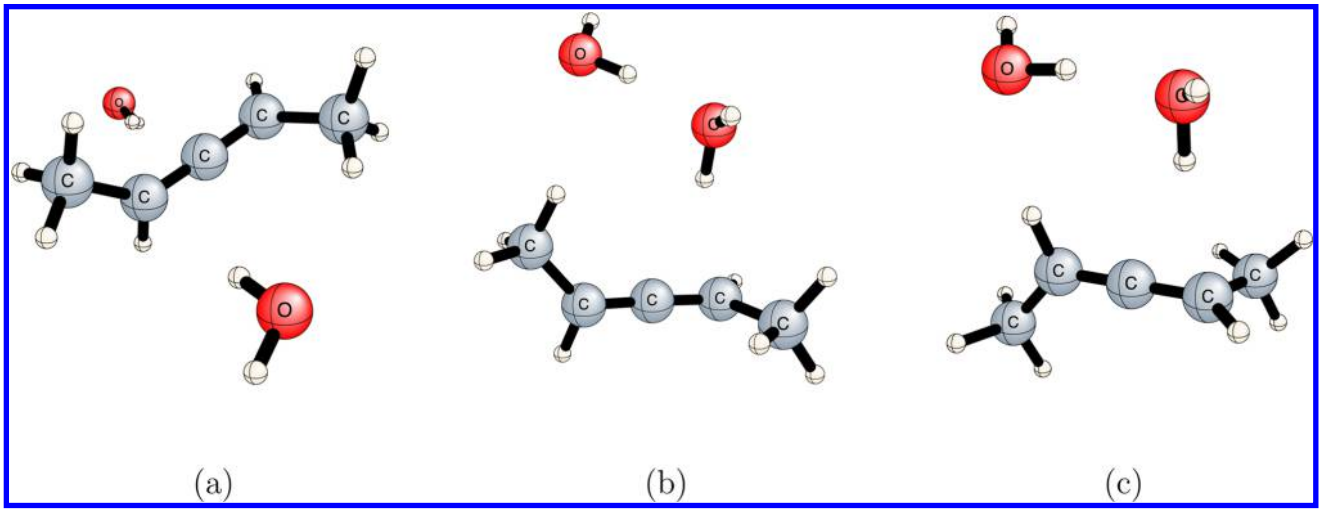

Figure 2. Test configurations of (*P*)-dimethylallene interacting with two water molecules, as optimized at the B3LYP/aug-cc-pVDZ level of theory.

3. COMPUTATIONAL DETAILS

Selected configurations of (*P*)-dimethylallene interacting with small numbers of water molecules were optimized using the B3LYP density functional[67−69] in conjunction with the correlation-consistent double-ζ basis set augmented with diffuse *s*- and *p*-type orbitals (aug-cc-pVDZ) developed by Dunning and co-workers.[70,71] To ensure reproducibility of the reported specific rotations, we employed tight convergence criteria with maximum values of 10^{-7} E_h/a_0 for both the individual Cartesian components and the root-mean-squared value of the energy gradient (all structures are provided in the Supporting Information.) In addition, we confirmed that all structures are minima on their respective potential surfaces via quadratic force constant analysis. Structural optimizations and vibrational analyses were carried our using the Gaussian09 quantum chemistry program.[72]

For each optimized structure, we computed specific rotations (in deg dm^{-1} $(g/mL)^{-1}$) of plane-polarized at four wavelengths—633, 589, 436, and 355 nm—employing linear-response theory with the second-order coupled cluster method (CC2)[73−75] and the aug-cc-pVDZ basis set. The carbon and oxygen 1*s* core orbitals were kept frozen in all coupled cluster response computations. The specific rotation was obtained using eq 2. However, to directly compare the specific rotations in the presence of explicit solvent molecules vs frozen-density embedding potentials, the trace of the $\mathbf{G}'$ tensor corresponding to the solvent molecules alone (in the same orientation as in the supermolecule) was subtracted from that of the full system, and only the mass of the (*P*)-dimethylallene solute was included in eq 2. Thus, for the conversion of the Rosenfeld tensor trace to the specific rotation, the mass of the solvent molecules, for instance, was ignored. This allows us to maintain the familiar units of specific rotation and provides a more meaningful comparison between rotations for systems with different numbers of solvent molecules. All coupled cluster computations were carried out using the PSI4 electronic structure package.[76]

All frozen-density embedding (FDE) potential[66,77,78] computations were carried out using release 2012.01 of the Amsterdam Density Functional (ADF) program system.[79,80] The FDE potential was computed using the PW91k[81,82] nonadditive kinetic-energy component and the exchange-correlation potential of the PBE density functional with the Slater type TZP basis set provided by ADF, employing five relaxation cycles to ensure convergence of the FDE freeze−thaw procedure. The resulting potential was then represented on a weighted three-dimensional numerical grid and then transferred to the PSI4 package where it was transformed to the same aug-cc-pVDZ basis set used for the coupled cluster linear response computations via

DOI: 10.1021/acs.jctc.5b00845
J. Chem. Theory Comput. 2015, 11, 5305−5315

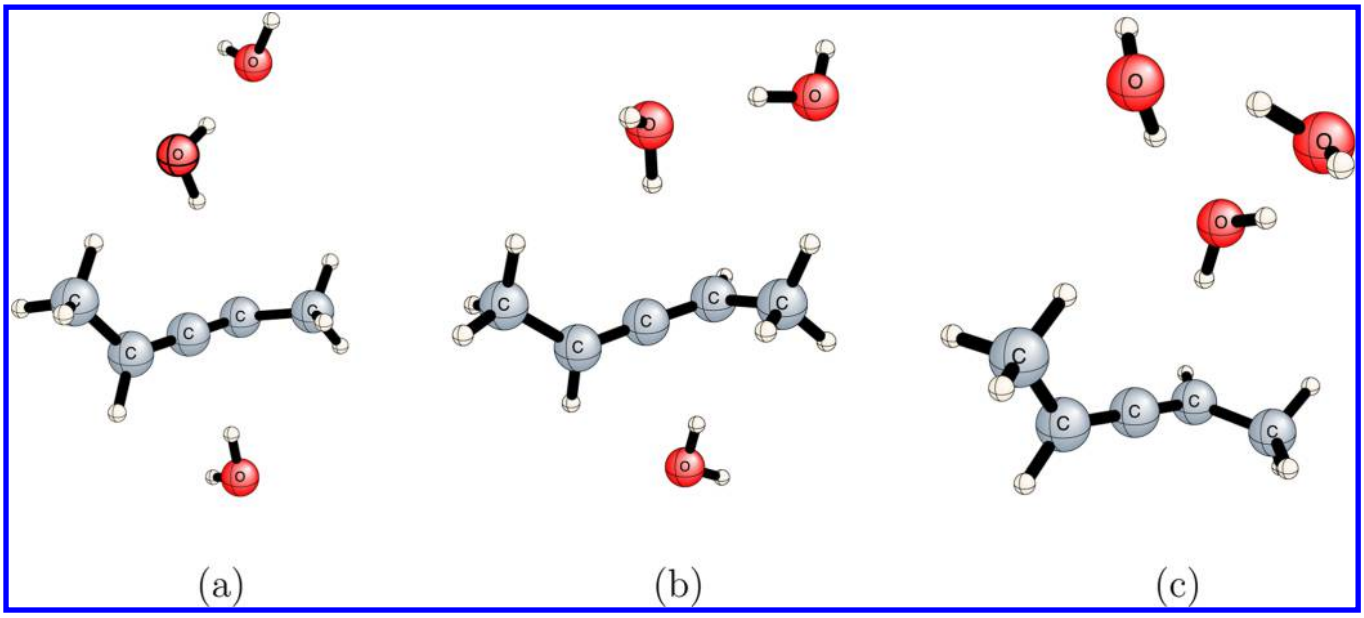

Figure 3. Test configurations of (*P*)-dimethylallene interacting with three water molecules, as optimized at the B3LYP/aug-cc-pVDZ level of theory.

$$v_{ij} = \langle \phi_i | v_{\text{eff}}^{\text{emb}}(\mathbf{r}) | \phi_j \rangle \approx \sum_k w_k v_{\text{eff}}^{\text{emb}}(\mathbf{r}_k) \phi_i(\mathbf{r}_k) \phi_j(\mathbf{r}_k) \quad (6)$$

where $\phi_i(\mathbf{r}_k)$ denotes the value of the basis function i at k-th grid point. The final potential was then added to the (*P*)-dimethylallene molecular Hamiltonian for the subsequent optical rotation computation.

4. RESULTS AND DISCUSSION

Figures 1, 2, and 3 depict optimized configurations of (*P*)-dimethylallene interacting with one, two, or three water molecules, respectively. These structures are by no means intended to provide an exhaustive set of optimized configurations but are merely a representative sample of microsolvated structures that illustrate both the weak and strong perturbations typically produced by individual solvent molecules on the chiroptical properties of a common solute such as (*P*)-dimethylallene.

The intermolecular interaction between the water molecules and (*P*)-dimethylallene in all of the structures considered here occurs between one of the hydrogens of a water molecule and the π system of the allene group and thus favors the end of the molecule in which the terminal methyl carbon lies in the same plane as the C═C═C moiety. These structures exhibit interaction energies ranging from roughly 2.5 kcal/mol (at the B3LYP/aug-cc-pVDZ level of theory) for one water molecule to more than 17 kcal/mol for three water molecules, depending on the number of interactions between the dimethylallene π system relative to hydrogen bonds between the solvent species. These results are in reasonable agreement with the much more exhaustive computations of Tschumper and co-workers,[83] who determined the interaction energy of the isolated water trimer to be 15.8 kcal/mol.

Wiberg et al.[38] reported both experimental and theoretical specific rotations of (*P*)-dimethylallene in 2008. Their condensed-phase measurements included both the neat state and a variety of polar and nonpolar solvents (exhibiting only minor variations in the results with the choice of solvent), whereas their gas-phase data were obtained using the novel cavity-ring-down polarimetry (CRDP) approach devised by Vaccaro and co-workers.[30,84] Figure 4 compares the neat-state and gas-phase experimental specific rotations of Wiberg et al.

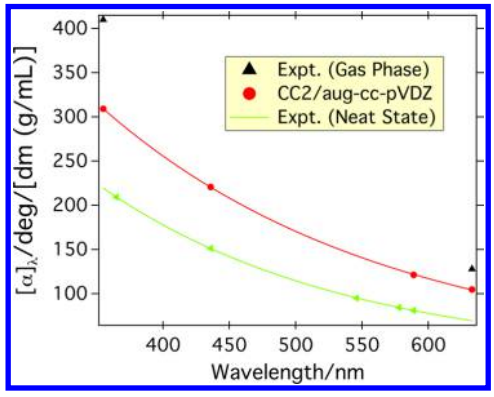

Figure 4. Theoretical (aug-cc-pVDZ/CC2) and experimental (in vacuum and neat state) optical rotatory dispersion of (*P*)-dimethylallene in configurations of (*P*)-dimethylallene. Experimental values taken from ref 38.

with the aug-cc-pVDZ/CC2 results computed in this work. In agreement with the analysis of ref 38, modified velocity-gauge coupled cluster specific rotations agree much more closely with the gas-phase CRDP data than their condensed-phase counterparts. In addition to norbornenone,[48,85] (*P*)-dimethylallene represents yet another example for which gas- and condensed-phase specific rotations differ substantially with more polar solvents yielding results somewhat closer to the vapor than nonpolar solvents as opposed to conventional chemical intuition.

The specific rotation of (*P*)-dimethylallene interacting with one, two, and three water molecules is given in Figures 5, 6, and 7, respectively, where the three plots in each figure correspond to the optimized configurations shown in Figures 1, 2, and 3, respectively. The red curves in the figures were obtained by explicit inclusion of the water molecules in the coupled cluster response calculation, and the blue curves correspond to use of DFT-based FDE potentials to represent the solute−water

DOI: 10.1021/acs.jctc.5b00845
J. Chem. Theory Comput. 2015, 11, 5305−5315

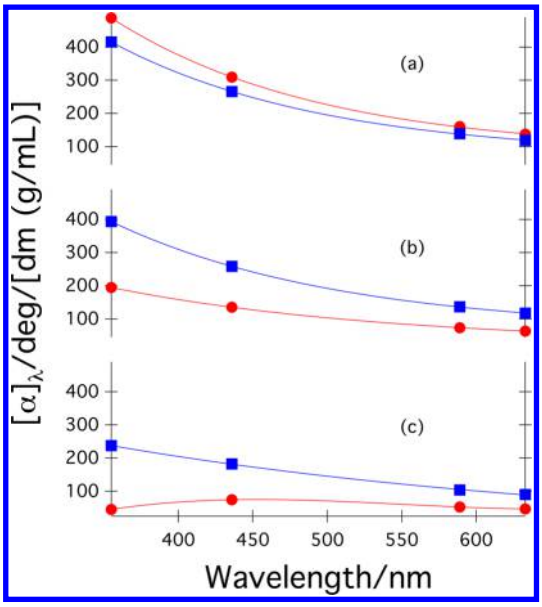

Figure 5. Specific rotation (aug-cc-pVDZ/CC2) as a function of wavelength for configurations of (*P*)-dimethylallene interacting with one water molecule. Plots (a), (b), and (c) correspond to the structures given in Figure 1. The red curves correspond to computations explicitly including the water molecules, whereas the blue curves were obtained using FDE potentials to represent the solvent molecules.

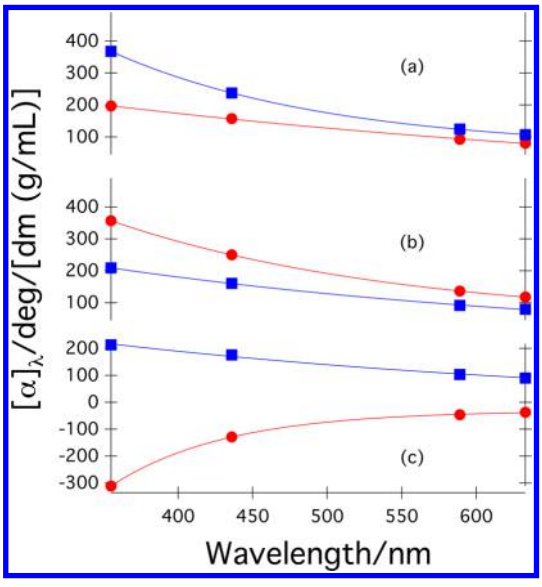

Figure 6. Specific rotation (aug-cc-pVDZ/CC2) as a function of wavelength for configurations of (*P*)-dimethylallene interacting with two water molecules. Plots (a), (b), and (c) correspond to the structures given in Figure 2. The red curves correspond to computations explicitly including the water molecules, whereas the blue curves were obtained using FDE potentials to represent the solvent molecules.

interaction. Corresponding numerical data are provided in Table S11 of the Supporting Information.

In all three single-water configurations, the introduction of an explicit water molecule produces a significant shift in the computed specific rotation as compared to the vacuum. For example, for structure 1(a), the 355 nm specific rotation is 487 as compared to 309 deg dm^{-1} $(g/mL)^{-1}$ in vacuum (cf. Figure 4). Similarly large variations are exhibited in the explicitly solvated two- and three-water configurations of Figures 2 and 3, respectively. However, the most striking results are the clear *qualitative* change to the shape of the specific rotation dispersion curve relative to the vacuum introduced by the water molecule in configuration 1(c) and the pair of water molecules in configuration 2(c). In both of these cases, the solvent molecules appear to introduce a reversal of the sign of the Cotton effect; however, as will be shown later, the sign is actually unchanged, but the *onset* of the effect is shifted to significantly longer wavelengths of polarized light. Nevertheless, these large shifts are representative of the challenges in describing accurately the impact of solvent on chiroptical properties.

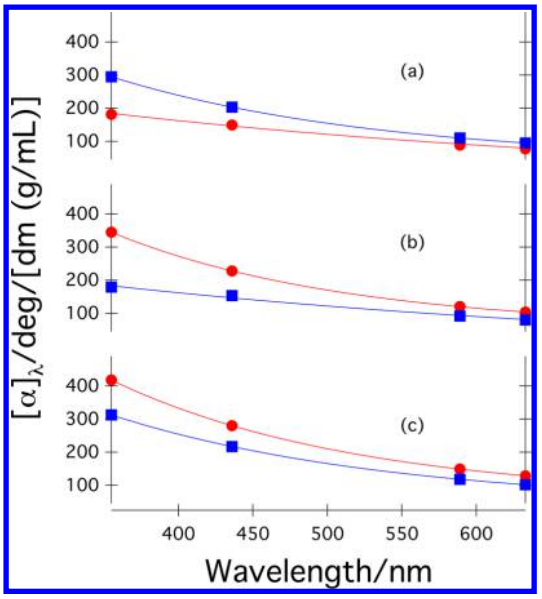

Figure 7. Specific rotation (aug-cc-pVDZ/CC2) as a function of wavelength for configurations of (*P*)-dimethylallene interacting with three water molecules. Plots (a), (b), and (c) correspond to the structures given in Figure 3. The red curves correspond to computations explicitly including the water molecules, whereas the blue curves were obtained using FDE potentials to represent the solvent molecules.

Unfortunately, the large solvent perturbations apparent in the explicitly solvated computations are not reproduced by the FDE potentials, as shown by the blue curves of Figures 5–7. In each of the test cases involving one or more water molecules, the FDE shifts are either much smaller than or in the opposite direction of the corresponding explicit-solvation results. For example, for configuration 1(c), the 355 nm specific rotation obtained using the FDE potential is 237 deg dm^{-1} $(g/mL)^{-1}$, clearly a decrease relative to the gas-phase calculation of 309 deg dm^{-1} $(g/mL)^{-1}$. However, although the direction of the shift is correct, the magnitude is far too small as compared to the explicitly solvated result of 45 deg dm^{-1} $(g/mL)^{-1}$. Similarly for structure 2(c), the FDE potential insufficiently decreases the specific rotation at each wavelength, as even the longest wavelength (633 nm) specific rotation calculated with explicit solvation is already opposite in sign as compared to the vacuum rotation. Furthermore, for test configurations 1(b), 2(a), 2(b), and 3(b), the FDE potentials produce shifts in the specific rotation curves in the opposite direction from their explicitly solvated counterparts.

DOI: 10.1021/acs.jctc.5b00845
J. Chem. Theory Comput. 2015, 11, 5305−5315

Insight into the nature of the discrepancies between the ORD response of (*P*)-dimethylallene using the FDE potential and explicit solvation can be obtained by examination of the corresponding UV absorption and electronic circular dichroism spectra. Figures 8, 9, and 10 depict such spectra for

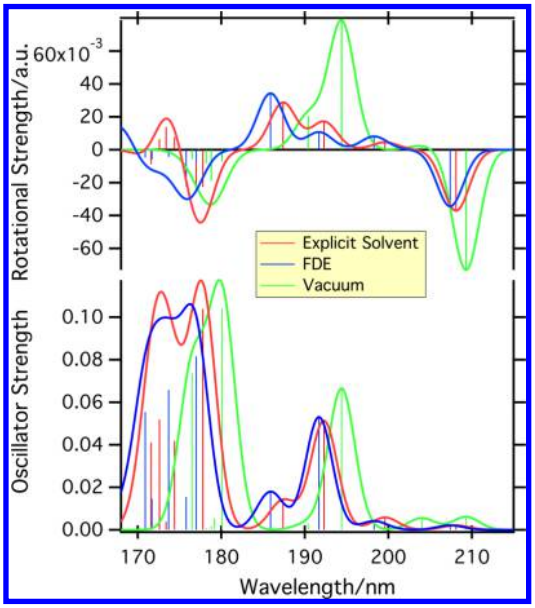

Figure 8. ECD (top) and UV absorption (bottom) spectra simulated at the aug-cc-pVDZ/CC2 level of theory for (*P*)-dimethylallene in vacuum (green) and the optimized structure in Figure 1(a) with one water molecule included explicitly (red) or via FDE potential (blue).

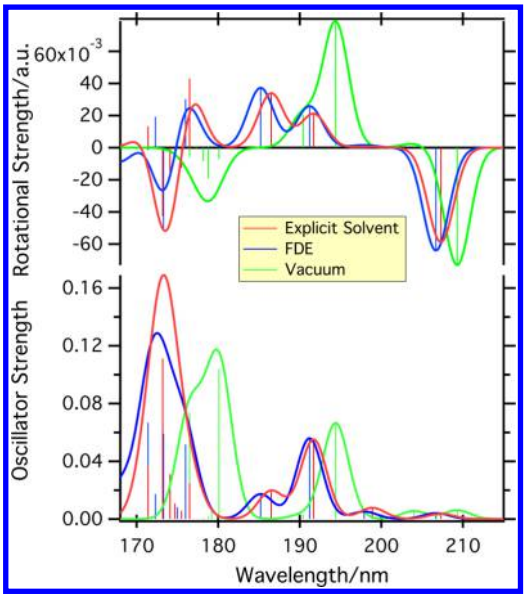

Figure 9. ECD (top) and UV absorption (bottom) spectra simulated at the aug-cc-pVDZ/CC2 level of theory for (*P*)-dimethylallene in vacuum (green) and the optimized structure in Figure 1(c) with one water molecule included explicitly (red) or via FDE potential (blue).

configurations 1(a), 1(c), and 2(c), respectively, as well as for the isolated solute. In addition, Table 1 reports the contribution of the first ten electronically excited states to the total specific rotation at the sodium D-line for each of these four systems (oscillator strengths are collected in Table S12).

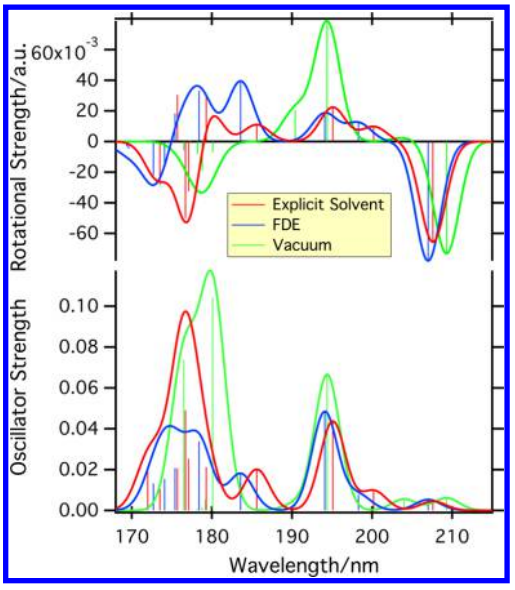

Figure 10. ECD (top) and UV absorption (bottom) spectra simulated at the aug-cc-pVDZ/CC2 level of theory for (*P*)-dimethylallene in vacuum (green) and the optimized structure in Figure 2(c) with two water molecules included explicitly (red) or via FDE potential (blue).

The UV and ECD spectra of gas-phase (*P*)-dimethylallene exhibit three transitions below 6.4 eV at 209.3, 204.0, and 194.4 nm that may be assigned as 1 ^1B, 2 ^1A, and 2 ^1B, respectively, in C_2 symmetry. These states correspond to the $^1A_2$, $^1B_1$, and $^1B_2$ transitions in the parent (D_{2d}) allene, as discussed in detail by Rauk, Drake, and Mason.[86] We find that each of these states exhibits both valence $\pi \rightarrow \pi^*$ and $\pi \rightarrow 3s$ Rydberg character. Although the gas-phase experimental CD spectrum of (*P*)-dimethylallene reported by Rauk and co-workers (for the *M* enantiomer) exhibits two bands at approximately 5.6 and 6.17 eV with the same rotatory strength, we find that the second band has the opposite sign of its lower-energy counterpart. Only at much shorter polarized wavelengths (below 350 nm) does the negative rotatory strength of the 1 ^1B state finally dominate the specific rotation of gas-phase (*P*)-dimethylallene. A fourth state (3 ^1A) near 190 nm (6.5 eV) also contributes to the positive long-wavelength Cotton signal, though its rotatory strength is less than one-third that of its larger neighbor. Higher-energy transitions near 6.9 eV and above exhibit negative rotatory strengths, apart from two very weak *A* transitions that are swamped out by their stronger *B*-irrep counterparts. These same higher-energy transitions have large oscillator strengths that, in fact, dominate the UV absorption spectrum. Rauk and co-workers noted, however, that bands above 6.7 eV must be responsible for the overall sign of the sodium D-line specific rotation of (*P*)-dimethylallene, given that their observed lowest-energy bands have the opposite sign. Our computations agree qualitatively with this interpretation, as we find a series of higher-energy bands with positive rotatory strengths (cf. Figure 4) that offset the negative contributions of states five through ten and ultimately yield the observed positive specific rotation.

The red spectra in Figures 8 and 9 reveal that the introduction of a single, explicit water molecule in configurations 1(a) and 1(c), respectively, produce a slight blue shift in every peak in the UV and ECD spectra above 170 nm. Although some peaks are damped by the perturbation (e.g., the lowest-energy, negative peak in Figure 8), others are magnified

DOI: 10.1021/acs.jctc.5b00845
J. Chem. Theory Comput. 2015, 11, 5305−5315

Table 1. Excitation Energy (eV), Excitation Wavelength (nm), Rotatory Strength (10^{-40} esu^2 cm^2, Velocity Gauge), and Optical Rotation Contribution (deg dm^{-1} (g/mL)$^{-1}$) for First 10 Excited States of (*P*)-Dimethylallene at the CC2/aug-cc-pVDZ Level of Theory for the Isolated Molecule As Compared to Microsolvated Structures 1(a), 1(c), and 2(c) Using Either Explicit Water Molecules (Upper Group) or FDE Potentials (Lower Group)

explicit water molecules															
vacuum				structure 1(a)				structure 1(c)				structure 2(c)			
ΔE_i	λ_i	R_i	$[\alpha]_D^i$	ΔE_i	λ_i	R_i	$[\alpha]_D^i$	ΔE_i	λ_i	R_i	$[\alpha]_D^i$	ΔE_i	λ_i	R_i	$[\alpha]_D^i$
5.924	209.3	−34.46	−668.18	5.959	208.1	−17.49	−334.65	5.980	207.3	−27.65	−524.78	5.973	207.6	−31.52	−599.71
6.079	204.0	1.20	21.86	6.212	199.6	2.11	36.66	6.232	198.9	0.23	3.94	6.194	200.2	4.59	80.36
6.378	194.4	36.73	602.40	6.448	192.3	7.99	127.92	6.466	191.7	9.89	157.33	6.356	195.1	10.42	172.26
6.511	190.4	9.66	151.26	6.617	187.4	13.50	203.90	6.646	186.6	15.96	238.76	6.681	185.6	5.21	77.08
6.885	180.1	−3.35	−46.39	6.973	177.8	−10.66	−143.47	7.024	176.5	20.26	268.23	6.916	179.3	13.71	187.89
6.917	179.2	0.05	0.66	7.003	177.0	−11.79	−157.20	7.063	175.5	−5.89	−77.05	7.003	177.0	−14.97	−199.46
6.933	178.8	−8.95	−121.92	7.111	174.4	3.69	47.58	7.097	174.7	−1.81	−23.37	7.015	176.7	−23.60	−313.37
6.956	178.2	−3.97	−53.76	7.149	173.4	6.51	82.89	7.120	174.1	−7.13	−91.64	7.056	175.7	14.38	188.54
6.992	177.3	0.33	4.41	7.184	172.6	3.06	38.55	7.158	173.2	−20.13	−255.69	7.147	173.5	−13.32	−169.84
7.023	176.5	−2.72	−36.06	7.227	171.6	−4.20	−52.25	7.232	171.4	6.28	77.94	7.209	172.0	−0.45	−5.62
FDE potentials															
vacuum				structure 1(a)				structure 1(c)				structure 2(c)			
ΔE_i	λ_i	R_i	$[\alpha]_D^i$	ΔE_i	λ_i	R_i	$[\alpha]_D^i$	ΔE_i	λ_i	R_i	$[\alpha]_D^i$	ΔE_i	λ_i	R_i	$[\alpha]_D^i$
5.924	209.3	−34.46	−668.18	5.977	207.4	−16.20	−307.80	5.997	206.7	−30.29	−571.06	5.990	207.0	−36.98	−699.07
6.079	204.0	1.20	21.86	6.252	198.3	3.81	65.34	6.266	197.9	0.73	12.50	6.251	198.3	5.75	98.76
6.378	194.4	36.73	602.40	6.466	191.7	5.05	80.32	6.484	191.2	12.19	192.65	6.387	194.1	8.66	141.55
6.511	190.4	9.66	151.26	6.669	185.9	16.15	239.84	6.693	185.2	17.65	260.04	6.754	183.6	18.55	267.73
6.885	180.1	−3.35	−46.39	7.006	177.0	−3.63	−48.28	7.043	176.0	14.18	186.63	6.949	178.4	15.66	212.36
6.917	179.2	0.05	0.66	7.054	175.8	−10.45	−137.07	7.086	175.0	1.29	16.79	7.067	175.4	8.41	109.87
6.933	178.8	−8.95	−121.92	7.138	173.7	−2.01	−25.65	7.155	173.3	−23.58	−299.75	7.122	174.1	−6.74	−86.58
6.956	178.2	−3.97	−53.76	7.222	171.7	−2.79	−34.74	7.197	172.3	9.06	113.76	7.180	172.7	−10.42	−131.42
6.992	177.3	0.33	4.41	7.256	170.9	−2.25	−27.70	7.232	171.4	−0.72	−8.92	7.311	169.6	−2.23	−27.06
7.023	176.5	−2.72	−36.06	7.391	167.8	7.12	84.31	7.388	167.8	−4.25	−50.36	7.320	169.4	−1.50	−18.17

J. Chem. Theory Comput. 2015, 11, 5305−5315 DOI: 10.1021/acs.jctc.5b00845

slightly (e.g., the 190 nm peak in the same figure) due to the strong structural dependence of the chiroptical response, which is well-known.[2,4,31,44,87] The shorter-wavelength transitions below 180 nm vary more significantly, exhibiting qualitative differences in the CD spectrum as compared to the vacumm state. Furthermore, when two water molecules are introduced, the short-wavelength region of the spectrum diverges even more. As shown in Figure 10, the ECD spectrum for structure 2(c) exhibits all negative peaks for the isolated (*P*)-dimethylallene but alternating positive and negative peaks for the explicit-water calculation.

At longer wavelengths, the qualitative trends in the ECD spectra are reproduced correctly by the FDE potentials, as shown by the blue curves in the figures. For shorter wavelengths, however, the differences between the explicitly solvated and FDE spectra are more substantial, particularly in the sign patterns of the ECD peaks. For example, in Figure 8, both the vacuum and FDE-based spectra exhibit only negative rotatory strengths, whereas the explicitly solvated spectrum has both negative and positive peaks. For the spectrum of structure 1(c) in Figure 9, the FDE and explicit-water responses are much closer, and both are qualitatively different from the gas-phase spectrum in this region. Finally, for Figure 10 corresponding to structure 2(c), the FDE potential produces a qualitative agreement with explicit solvation only at wavelengths longer than 190 nm. The large negative peak at 176 nm is missing entirely, which is consistent with the wrong sign of the FDE specific rotation for this water configuration.

The numerical data in Table 1 also reveal the exceedingly slow convergence of the specific rotation with the number of states incuded in the Rosenfeld tensor in eq 1. For the isolated molecule, for example, the sodium D-line specific rotation at the CC2/aug-cc-pVDZ level of theory is +121.2 deg dm^{-1} $(g/mL)^{-1}$, whereas the sum of the contributions from the first ten excitations in the table is −145.7 deg dm^{-1} $(g/mL)^{-1}$. Similarly, for structure 1(c), the explicit CCLR calculation gives $[\alpha]_D$ = 52.4 deg dm^{-1} $(g/mL)^{-1}$, whereas the corresponding sum over the first ten states gives −226.3 deg dm^{-1} $(g/mL)^{-1}$ (expanding this sum to 30 states yields 299.5 deg dm^{-1} $(g/mL)^{-1}$). This observation is in accordance with the earlier analysis of Wiberg and co-workers[33] who reported that, for DFT-based ORD calculations, the sum over states expression converges only after inclusion of hundreds of excited states. Given the sensitivity of the ECD rotatory strength of each state to the solvent field, the errors in the model used to represent the solvent perturbation become magnified in the ORD.

The poor performance of the FDE approach in relation to the explicit solvation approach can be due to a number of approximations. In the FDE method, the environment is treated as electronically frozen, which means that both the solvent response and solvent-to-solute charge-transfer induced by the perturbing field are neglected.[64] Solute-to-solvent charge-transfer is possible as long as the basis of the solute is sufficiently flexible to describe such excitations. Another error is introduced by the density functional approximation to the exact kinetic energy functional. Of importance is the functional derivative of this term as this provides the kinetic-energy component to the embedding potential. The PW91k functional employed here has been studied for different molecular properties and is known to be somewhat too repulsive in the outer region of the solvent molecules and not repulsive enough in the inner core region.[88] The quality of this approximation can be indirectly judged by looking at the low-energy region of the ECD and UV absorption spectra in Figures 8 and 9. In this region, the effect of water excitations (which start at wavelengths shorter than ∼160 nm) is small. Given the semiquantitative agreement for the solvent-induced shifts for wavelengths above 190 nm, one may conclude that the PW91k approximation to the embedding potential is sufficiently accurate.

The other sources of error can partially be assessed by comparing FDE calculations with a more advanced treatment in which a limited number of excitations of the solvent water molecules are coupled to those of the solute. This is possible at the DFT level of theory, and we have carried out exploratory ADF calculations for configuration 2(c) (which exhibits the largest discrepancy between the FDE and explicit-solvation calculations). Using the TZ2P basis on both (*P*)-dimethylallene and water and the SAOP[89] XC functional to ensure a correct treatment of Rydberg excitations,[90] we find only small differences in the calculated CD spectrum between the coupled and uncoupled FDE approach. The largest shift (−36 meV) occurs for an excitation at 7.77 eV, which is close to the second water excitation at 7.80 eV. This small redshift is accompanied by a redistribution of the oscillator strength over the two water and one (*P*)-dimethylallene excitations that are mixed due to the coupling. The next step would be to compare the coupled FDE results with supermolecular DFT results, but this is complicated by the difficulty in determining the correct energy for charge-transfer excitations in DFT. The adiabatic LDA approximation used in the SAOP functional gives too low energies for charge-transfer states and increases the number of states below 7 eV from 6 in the coupled FDE to 10 in the supermolecular calculation. These additional states change the CD spectrum dramatically relative to the coupled FDE result. Although the low energy of the additional states is unphysical, this calculation illustrates the magnitude of errors that occur due to the neglect of charge transfer in the FDE approach. Furthermore, the correct inclusion of higher-energy charge-transfer states is probably essential due to the slow convergence of the optical rotation (cf. the last column of Table 1) in the sum-over-states formalism. This lack of charge-transfer excitations is thus likely to be the major cause for the observed discrepancy between the FDE and the explicit solvation calculations.

5. CONCLUSIONS

We have investigated the performance of a WFT-in-DFT FDE approach for computing properties, such as optical rotations and electronic circular dichroism spectra, using a test case of (*P*)-dimethylallene interacting with a limited number of water molecules in optimized configurations. The potential function arising from the solvent molecules is first computed using DFT and subsequently used for a coupled cluster linear response computation of the solvent within the solvated environment. Although this approach has seen considerable success in treating UV/vis spectra, it is far less amenable to the chiroptical properties considered here. Indeed, for several of the configurations of water and (*P*)-dimethylallene, the FDE potential yields too small a perturbation compared to an explicit "supermolecule" calculation, and for certain configurations, fails to reproduce the change in sign of the ORD introduced by the molecule-specific solute−solvent interactions. We have traced these errors primarily to the lack of solvent response to the external field—a factor that is pivotal for such nonadditive properties as ORD and ECD. Future

DOI: 10.1021/acs.jctc.5b00845
J. Chem. Theory Comput. 2015, 11, 5305−5315

development should therefore focus on effective and efficient means of incorporating the response of the solvent into the FDE computation. In principle, a recipe exists for determining these couplings, though no WFT-in-DFT implementation yet exists.[91]

■ ASSOCIATED CONTENT

Supporting Information

The Supporting Information is available free of charge on the ACS Publications website at DOI: 10.1021/acs.jctc.5b00845.

The B3LYP/aug-cc-pVDZ optimized geometries of isolated (*P*)-dimethylallene and the nine explicitly solvated structures shown in Figures 1−3 are given in Tables S1−S10; additionally, specific optical rotations of all structures are provided in Table S11, and the oscillator strengths for the lowest ten excited states of all structures are given in Table S12 (PDF)

■ AUTHOR INFORMATION

Corresponding Author

*E-mail: crawdad@vt.edu.

Notes

The authors declare no competing financial interest.

■ ACKNOWLEDGMENTS

This research was supported by Grants CHE-1465149 and ACI-1450169 from the U.S. National Science Foundation.

■ REFERENCES

(1) Barron, L. D. *Molecular Light Scattering and Optical Activity*, 2nd ed.; Cambridge University Press: Camridge, U.K., 2004.

(2) Pecul, M.; Ruud, K. The Ab Initio Calculation of Optical Rotation and Electronic Circular Dichroism. *Adv. Quantum Chem.* **2005**, *50*, 185−212.

(3) Crawford, T. D. *Ab Initio* Calculation of Molecular Chiroptical Properties. *Theor. Chem. Acc.* **2006**, *115*, 227−245.

(4) Crawford, T. D.; Tam, M. C.; Abrams, M. L. The Current State of *Ab Initio* Calculations of Optical Rotation and Circular Dichroism Spectra. *J. Phys. Chem. A* **2007**, *111*, 12057−12068.

(5) Crawford, T. D. In *Comprehensive Chiroptical Spectroscopy*; Berova, N., Nakanishi, K., Woody, R. W., Polavarapu, P., Eds.; Wiley: Hoboken, NJ, 2012; Vol. *1*; Chapter 23, pp 675−697.

(6) Cheeseman, J. R.; Frisch, M. J.; Devlin, F. J.; Stephens, P. J. Hartree-Fock and density functional theory ab initio calculation of optical rotation using GIAOs: Basis set dependence. *J. Phys. Chem. A* **2000**, *104*, 1039−1046.

(7) Furche, F.; Ahlrichs, R.; Wachsmann, C.; Weber, E.; Sobanski, A.; Vögtle, F.; Grimme, S. Circular dichroism of helicenes investigated by time-dependent density functional theory. *J. Am. Chem. Soc.* **2000**, *122*, 1717−1724.

(8) Stephens, P. J.; Devlin, F. J.; Cheeseman, J. R.; Frisch, M. J. Calculation of optical rotation using density functional theory. *J. Phys. Chem. A* **2001**, *105*, 5356−5371.

(9) Grimme, S. Calculation of frequency dependent optical rotation using density functional response theory. *Chem. Phys. Lett.* **2001**, *339*, 380−388.

(10) Stephens, P. J.; Devlin, F. J.; Cheeseman, J. R.; Frisch, M. J.; Rosini, C. Determination of Absolute Configuration Using Optical Rotation Calculated Using Density Functional Theory. *Org. Lett.* **2002**, *4*, 4595−4598.

(11) Grimme, S.; Furche, F.; Ahlrichs, R. An improved method for density functional calculations of the frequency-dependent optical rotation. *Chem. Phys. Lett.* **2002**, *361*, 321−328.

(12) Autschbach, J.; Patchkovskii, S.; Ziegler, T.; van Gisbergen, S.; Baerends, E. J. Chiroptical properties from time-dependent density functional theory. II. Optical rotation of small to medium sized organic molecules. *J. Chem. Phys.* **2002**, *117*, 581−592.

(13) Autschbach, J.; Ziegler, T.; van Gisbergen, S. J. A.; Baerends, E. J. Chiroptical properties from time-dependent density functional theory. I. Circular dichroism spectra of organic molecules. *J. Chem. Phys.* **2002**, *116*, 6930−6940.

(14) Autschbach, J.; Jorge, F. E.; Ziegler, T. Density functional calculations on electronic circular dichroism spectra of chiral transition metal complexes. *Inorg. Chem.* **2003**, *42*, 2867−2877.

(15) Ruud, K.; Helgaker, T. Optical rotation studied by density-functional and coupled-cluster methods. *Chem. Phys. Lett.* **2002**, *352*, 533−539.

(16) Ruud, K.; Stephens, P. J.; Devlin, F. J.; Taylor, P. R.; Cheeseman, J. R.; Frisch, M. J. Coupled-cluster calculations of optical rotation. *Chem. Phys. Lett.* **2003**, *373*, 606−614.

(17) Tam, M. C.; Russ, N. J.; Crawford, T. D. Coupled Cluster Calculations of Optical Rotatory Dispersion of (*S*)-Methyloxirane. *J. Chem. Phys.* **2004**, *121*, 3550−3557.

(18) Crawford, T. D.; Owens, L. S.; Tam, M. C.; Schreiner, P. R.; Koch, H. *Ab Initio* Calculation of Optical Rotation in (*P*)-(+)-[4]Triangulane. *J. Am. Chem. Soc.* **2005**, *127*, 1368−1369.

(19) Pulm, F.; Schramm, J.; Hormes, J.; Grimme, S.; Peyerimhoff, S. D. Theoretical and experimental investigations of the electronic circular dichroism and absorption spectra of bicyclic ketones. *Chem. Phys.* **1997**, *224*, 143−155.

(20) Kondru, R. K.; Wipf, P.; Beratan, D. N. Theory-Assisted Determination of Absolute Configuration for Complex Natural Products via Computation of Molar Rotation Angles. *J. Am. Chem. Soc.* **1998**, *120*, 2204−2205.

(21) Grimme, S.; Harren, J.; Sobanski, A.; Vögtle, F. Structure/Chiroptics Relationships of Planar Chiral and Helical Molecules. *Eur. J. Org. Chem.* **1998**, *1998*, 1491−1509.

(22) Polavarapu, P. L.; Chakraborty, D. K. Ab initio theoretical optical rotations of small molecules. *Chem. Phys.* **1999**, *240*, 1−8.

(23) Ribe, S.; Kondru, R. K.; Beratan, D. N.; Wipf, P. Optical Rotation Computation Total Synthesis, and Stereochemistry Assignment of the Marine Natural Product Pitiamide A. *J. Am. Chem. Soc.* **2000**, *122*, 4608−4617.

(24) Polavarapu, P. L. Optical Rotation: Recent Advances in Determining the Absolute Configuration. *Chirality* **2002**, *14*, 768−781.

(25) Diedrich, C.; Grimme, S. Systematic Investigation of Modern Quantum Chemical Methods to Predict Electronic Circular Dichroism Spectra. *J. Phys. Chem. A* **2003**, *107*, 2524−2539.

(26) Polavarapu, P. L.; Petrovic, A.; Wang, F. Intrinsic Rotation and Molecular Structure. *Chirality* **2003**, *15*, S143−S149.

(27) Diedrich, C.; Kausemann, S.; Grimme, S. Density functional calculations of the frequency-dependent optical rotation: Comparison of theory and experiment for the gas phase. *J. Comp. Meth. Sci. Eng.* **2004**, *4*, 1−8.

(28) Rinderspacher, B. C.; Schreiner, P. R. Structure-Property Relationships of Prototypical Chiral Compounds: Case Studies. *J. Phys. Chem. A* **2004**, *108*, 2867−2870.

(29) Stephens, P. J.; McCann, D. M.; Cheeseman, J. R.; Frisch, M. J. The Determination of Absolute Configurations of Chiral Molecules Using Ab Initio Time-Dependent Density Functional Theory Calculations of Optical Rotation: How Reliable Are Absolute Configurations Obtained for Molecules With Small Rotations? *Chirality* **2005**, *17*, S52−S64.

(30) Wilson, S. M.; Wiberg, K. B.; Cheeseman, J. R.; Frisch, M. J.; Vaccaro, P. H. The nonresonant optical activity of isolated organic molecules. *J. Phys. Chem. A* **2005**, *109*, 11752−11764.

(31) Wiberg, K. B.; Wang, Y.-G.; Vaccaro, P. H.; Cheeseman, J. R.; Luderer, M. R. Conformation Effects on Optical Rotation. 2-Substituted Butanes. *J. Phys. Chem. A* **2005**, *109*, 3405−3410.

(32) Wiberg, K. B.; Wang, Y.; Wilson, S. M.; Vaccaro, P. H.; Cheeseman, J. R. Chiroptical properties of 2-Chloropropionitrile. *J. Phys. Chem. A* **2005**, *109*, 3448−3453.

(33) Wiberg, K. B.; Wang, Y.; Wilson, S. M.; Vaccaro, P. H.; Cheeseman, J. R. Sum-over-states calculation of the specific rotations

DOI: 10.1021/acs.jctc.5b00845
J. Chem. Theory Comput. 2015, 11, 5305−5315

of some substituted oxiranes, chloropropionitrile, ethane, and norbornenone. *J. Phys. Chem. A* **2006**, *110*, 13995−14002.
(34) Tam, M. C.; Crawford, T. D. *Ab Initio* Determination of Optical Rotatory Dispersion in the Conformationally Flexible Molecule (*R*)-Epichlorohydrin. *J. Phys. Chem. A* **2006**, *110*, 2290−2298.
(35) Kowalczyk, T. D.; Abrams, M. L.; Crawford, T. D. *Ab Initio* Optical Rotatory Dispersion and Electronic Circular Dichroism Spectra of (*S*)-2-Chloropropionitrile. *J. Phys. Chem. A* **2006**, *110*, 7649−7654.
(36) Crawford, T. D.; Tam, M. C.; Abrams, M. L. The problematic case of (*S*)-methylthiirane: Electronic Circular Dichroism Spectra and Optical Rotatory Dispersion. *Mol. Phys.* **2007**, *105*, 2607−2617.
(37) Tam, M. C.; Abrams, M. L.; Crawford, T. D. Chiroptical properties of (*R*)-3-chloro-1-butene and (*R*)-2-chlorobutane. *J. Phys. Chem. A* **2007**, *111*, 11232−11241.
(38) Wiberg, K. B.; Wang, Y.; Wilson, S. M.; Vaccaro, P. H.; Jorgensen, W. L.; Crawford, T. D.; Abrams, M. L.; Cheeseman, J. R.; Luderer, M. Optical Rotatory Dispersion of 2,3-Hexadiene and 2,3-Pentadiene. *J. Phys. Chem. A* **2008**, *112*, 2415−2422.
(39) Crawford, T. D.; Stephens, P. J. A Comparison of Time-Dependent Density-Functional Theory and Coupled Cluster Theory for the Calculation of the Optical Rotations of Chiral Molecules. *J. Phys. Chem. A* **2008**, *112*, 1339−1345.
(40) Pedersen, T. B.; Kongsted, J.; Crawford, T. D. Gas Phase Optical Rotation Calculated from Coupled Cluster Theory with Zero-Point Vibrational Corrections from Density Functional Theory. *Chirality* **2009**, *21*, S68−S75.
(41) Crawford, T. D.; Allen, W. D. Optical activity in conformationally flexible molecules: A theoretical study of large-amplitude vibrational averaging in (*R*)-3-chloro-1-butene. *Mol. Phys.* **2009**, *107*, 1041−1057.
(42) Pedersen, T. B.; Kongsted, J.; Crawford, T. D.; Ruud, K. On the importance of vibrational contributions to small-angle optical rotation: Fluorooxirane in gas phase and solution. *J. Chem. Phys.* **2009**, *130*, 034310.
(43) Crawford, T. D. In *Recent Progress in Coupled Cluster Methods: Theory and Applications*; Carsky, P., Pittner, J., Paldus, J., Eds.; Challenges and Advances in Computational Chemistry and Physics; Springer: Berlin, 2010; Vol. *11*; Chapter 2, pp 37−55.
(44) Autschbach, J. Computing Chiroptical Properties wth First-Principles Theoretical Methods: Background and Illustrative Examples. *Chirality* **2009**, *21*, E116−E152.
(45) Pritchard, B.; Autschbach, J. Calculation of the Vibrationally Resolved, Circularly Polarized Luminescence of d-Camphorquinone and (S,S)-trans-beta-Hydrindanone. *ChemPhysChem* **2010**, *11*, 2409−2415.
(46) Lambert, J. M.; Compton, R. N.; Crawford, T. D. The Optical Activity of Carvone: A Theoretical and Experimental Investigation. *J. Chem. Phys.* **2012**, *136*, 114512.
(47) Mach, T. J.; Crawford, T. D. Computing Optical Rotation via an *N*-Body Approach. *Theor. Chem. Acc.* **2014**, *133*, 1449.
(48) Lahiri, P.; Wiberg, K. B.; Vaccaro, P. H.; Caricato, M.; Crawford, T. D. Large Solvation Effect in the Optical Rotatory Dispersion of Norbornenone. *Angew. Chem., Int. Ed.* **2014**, *53*, 1386−1389.
(49) Neugebauer, J. Induced Chirality in Achiral Media — How Theory Unravels Mysterious Solvent Effects. *Angew. Chem., Int. Ed.* **2007**, *46*, 7738−7740.
(50) Mennucci, B.; Tomasi, J.; Cammi, R.; Cheeseman, J. R.; Frisch, M. J.; Devlin, F. J.; Gabriel, S.; Stephens, P. J. Polarizable continuum model (PCM) calculations of solvent effects on optical rotation of chiral molecules. *J. Phys. Chem. A* **2002**, *106*, 6102−6113.
(51) Pecul, M.; Marchesan, D.; Ruud, K.; Coriani, S. Polarizable continuum model study of solvent effects on electronic circular dichroism parameters. *J. Chem. Phys.* **2005**, *122*, 024106.
(52) Mukhopadhyay, P.; Zuber, G.; Goldsmith, M. R.; Wipf, P.; Beratan, D. N. Solvent effect on optical rotation: A case study of methyloxirane in water. *ChemPhysChem* **2006**, *7*, 2483−2486.
(53) Mukhopadhyay, P.; Zuber, G.; Wipf, P.; Beratan, D. N. Contribution of a solute's chiral solvent imprint to optical rotation. *Angew. Chem., Int. Ed.* **2007**, *46*, 6450−6452.
(54) Lipparini, F.; Egidi, F.; Cappelli, C.; Barone, V. The Optical Rotation of Methyloxirane in Aqueous Solution: A Never Ending Story? *J. Chem. Theory Comput.* **2013**, *9*, 1880−1884.
(55) Kongsted, J.; Pedersen, T. B.; Strange, M.; Osted, A.; Hansen, A. E.; Mikkelsen, K. V.; Pawlowski, F.; Jørgensen, P.; Hättig, C. Coupled cluster calculations of the optical rotation of *S*-propylene oxide in gas phase and solution. *Chem. Phys. Lett.* **2005**, *401*, 385−392.
(56) Kongsted, J.; Pedersen, T. B.; Jensen, L.; Hansen, A. E.; Mikkelsen, K. V. Coupled cluster and density functional theory study of the vibrational contribution to the optical rotation of (*S*)-propylene oxide. *J. Am. Chem. Soc.* **2006**, *128*, 976−982.
(57) Koch, H.; Christiansen, O.; Jørgensen, P.; de Merás, A. M. S.; Helgaker, T. The CC3 model: An iterative coupled cluster approach including connected triples. *J. Chem. Phys.* **1997**, *106*, 1808−1818.
(58) Christiansen, O.; Koch, H.; Jørgensen, P. Response functions in the CC3 iterative triple excitation model. *J. Chem. Phys.* **1995**, *103*, 7429−7441.
(59) Caricato, M. Implementation of the CCSD-PCM linear response function for frequency dependent properties in solution: Application to polarizability and specific rotation. *J. Chem. Phys.* **2013**, *139*, 114103.
(60) Wesolowski, T. A.; Warshel, A. Frozen density functional approach for ab initio calculations of solvated molecules. *J. Phys. Chem.* **1993**, *97*, 8050−8053.
(61) Wesolowski, T. A. In *Computational Chemistry: Reviews of Current Trends*; Leszczynski, J., Ed.; World Scientific: Singapore, 2006; Vol. *10*; pp 1−82.
(62) Govind, N.; Wang, Y. A.; da Silva, A. J. R.; Carter, E. A. Accurate ab initio energetics of extended systems via explicit correlation embedded in a density functional environment. *Chem. Phys. Lett.* **1998**, *295*, 129−134.
(63) Govind, N.; Wang, Y. A.; Carter, E. A. Electronic-structure calculations by first-principles density-based embedding of explicitly correlated systems. *J. Chem. Phys.* **1999**, *110*, 7677−7688.
(64) Neugebauer, J. On the calculation of general response properties in subsystem density functional theory. *J. Chem. Phys.* **2009**, *131*, 084104.
(65) Rosenfeld, L. Quantenmechanische Theorie der natürlichen optischen Aktivität von Flüssigkeiten und Gasen. *Eur. Phys. J. A* **1929**, *52*, 161−174.
(66) Jacob, C. R.; Neugebauer, J.; Visscher, L. A Flexible Implementation of Frozen-Density Embedding for Use in Multilevel Simulations. *J. Comput. Chem.* **2008**, *29*, 1011−1018.
(67) Becke, A. D. Density-functional thermochemistry. III. The role of exact exchange. *J. Chem. Phys.* **1993**, *98*, 5648−5652.
(68) Lee, C.; Yang, W.; Parr, R. G. Development of the Colle-Salvetti correlation-energy formula into a functional of the electron density. *Phys. Rev. B: Condens. Matter Mater. Phys.* **1988**, *37*, 785−789.
(69) Stephens, P. J.; Devlin, F. J.; Chabalowski, C. F.; Frisch, M. J. *Ab initio* Calculation of Vibrational Absorption and Circular Dichroism Spectra Using Density Functional Theory. *J. Phys. Chem.* **1994**, *98*, 11623−11627.
(70) Dunning, T. H. Gaussian basis sets for use in correlated molecular calculations. I. The atoms boron through neon. *J. Chem. Phys.* **1989**, *90*, 1007−1023.
(71) Woon, D. E.; Dunning, T. H. Gaussian basis sets for use in correlated molecular calculations. IV. Calculation of static electrical response properties. *J. Chem. Phys.* **1994**, *100*, 2975−2988.
(72) Frisch, M. J.; Trucks, G. W.; Schlegel, H. B.; Scuseria, G. E.; Robb, M. A.; Cheeseman, J. R.; Scalmani, G.; Barone, V.; Mennucci, B.; Petersson, G. A.; Nakatsuji, H.; Caricato, M.; Li, X.; Hratchian, H. P.; Izmaylov, A. F.; Bloino, J.; Zheng, G.; Sonnenberg, J. L.; Hada, M.; Ehara, M.; Toyota, K.; Fukuda, R.; Hasegawa, J.; Ishida, M.; Nakajima, T.; Honda, Y.; Kitao, O.; Nakai, H.; Vreven, T.; Montgomery, J.; Peralta, J. E.; Ogliaro, F.; Bearpark, M.; Heyd, J. J.; Brothers, E.; Kudin, K. N.; Staroverov, V. N.; Kobayashi, R.; Normand, J.; Raghavachari, K.;

DOI: 10.1021/acs.jctc.5b00845
J. Chem. Theory Comput. 2015, 11, 5305−5315

Rendell, A.; Burant, J. C.; Iyengar, S. S.; Tomasi, J.; Cossi, M.; Rega, N.; Millam, J. M.; Klene, M.; Knox, J. E.; Cross, J. B.; Bakken, V.; Adamo, C.; Jaramillo, J.; Gomperts, R.; Stratmann, R. E.; Yazyev, O.; Austin, A. J.; Cammi, R.; Pomelli, C.; Ochterski, J. W.; Martin, R. L.; Morokuma, K.; Zakrzewski, V. G.; Voth, G. A.; Salvador, P.; Dannenberg, J. J.; Dapprich, S.; Daniels, A. D.; Farkas, Ö; Foresman, J. B.; Ortiz, J. V.; Cioslowski, J.; Fox, D. J. *Gaussian 09*, revision A.1; Gaussian Inc.: Wallingford, CT, 2009.

(73) Christiansen, O.; Koch, H.; Jørgensen, P. The second-order approximate coupled cluster singles and doubles model CC2. *Chem. Phys. Lett.* **1995**, *243*, 409−418.

(74) Christiansen, O.; Jørgensen, P.; Helgaker, T. Integral direct calculation of CC2 excitation energies: singlet excited states of benzene. *Chem. Phys. Lett.* **1996**, *263*, 530−539.

(75) Koch, H.; Jørgensen, P. Coupled cluster response functions. *J. Chem. Phys.* **1990**, *93*, 3333−3344.

(76) Turney, J. M.; Simmonett, A. C.; Parrish, R. M.; Hohenstein, E. G.; Evangelista, F.; Fermann, J. T.; Mintz, B. J.; Burns, L. A.; Wilke, J. J.; Abrams, M. L.; Russ, N. J.; Leininger, M. L.; Janssen, C. L.; Seidl, E. T.; Allen, W. D.; Schaefer, H. F.; King, R. A.; Valeev, E. F.; Sherrill, C. D.; Crawford, T. D. PSI4: An Open-Source *Ab Initio* Electronic Structure Program. *Wiley Interdisciplinary Reviews: Computational Molecular Science* **2012**, *2*, 556−565.

(77) Neugebauer, J.; Jacob, C. R.; Wesolowski, T. A.; Baerends, E. J. An Explicit Quantum Chemical Method for Modeling Large Solvation Shells Applied to Aminocoumarin C151. *J. Phys. Chem. A* **2005**, *109*, 7805−7814.

(78) Gomes, A. S. P.; Jacob, C. R.; Visscher, L. Calculation of local excitations in large systems by embedding wave-function theory in density-functional theory. *Phys. Chem. Chem. Phys.* **2008**, *10*, 5353−5362.

(79) Amsterdam Density Functional program, Theoretical Chemistry. Vrije Universiteit, Amsterdam. http://www.scm.com.

(80) te Velde, G.; Bickelhaupt, F. M.; Baerends, E. J.; Guerra, C. F.; van Gisbergen, S. J. A.; Snijders, J. G.; Ziegler, T. Chemistry with ADF. *J. Comput. Chem.* **2001**, *22*, 931−967.

(81) Lembarki, A.; Chermette, H. Obtaining a gradient-corrected kinetic-energy functional from the Perdew-Wang exchange functional. *Phys. Rev. A: At., Mol., Opt. Phys.* **1994**, *50*, 5328−5331.

(82) Wesolowski, T.; Chermette, H.; Weber, J. Accuracy of approximate kinetic energy functionals in the model of Kohn-Sham equations with constrained electron density: The FH center dot center dot center dot NCH complex as a test case. *J. Chem. Phys.* **1996**, *105*, 9182−9190.

(83) Anderson, J. A.; Crager, K.; Federoff, L.; Tschumper, G. S. Anchoring the potential energy surface of the cyclic water trimer. *J. Chem. Phys.* **2004**, *121*, 11023−11029.

(84) Müller, T.; Wiberg, K. B.; Vaccaro, P. H. Cavity Ring-Down Polarimetry (CRDP): A New Scheme for Probing Circular Birefringence and Circular Dichroism in the Gas Phase. *J. Phys. Chem. A* **2000**, *104*, 5959−5968.

(85) Caricato, M.; Vaccaro, P. H.; Crawford, T. D.; Wiberg, K. B.; Lahiri, P. Insights on the Origin of the Unusually Large Specific Rotation of (*1S, 4S*)-Norbornenone. *J. Phys. Chem. A* **2014**, *118*, 4863−4871.

(86) Rauk, A.; Drake, A. F.; Mason, S. F. Excited States and Optical Activity of Allenes. Allene, 1,3-Dimethylallene, and 1,2-Cyclononadiene. *J. Am. Chem. Soc.* **1979**, *101*, 2284−2289.

(87) Wiberg, K. B.; Vaccaro, P. H.; Cheeseman, J. R. Conformational effects on optical rotation. 3-Substituted 1-butenes. *J. Am. Chem. Soc.* **2003**, *125*, 1888−1896.

(88) Fux, S.; Jacob, C. R.; Neugebauer, J.; Visscher, L.; Reiher, M. Accurate frozen-density embedding potentials as a first step towards a subsystem description of covalent bonds. *J. Chem. Phys.* **2010**, *132*, 164101.

(89) Schipper, P.; Gritsenko, O.; van Gisbergen, S.; Baerends, E. Molecular calculations of excitation energies and (hyper)-polarizabilities with a statistical average of orbital model exchange-correlation potentials. *J. Chem. Phys.* **2000**, *112*, 1344−1352.

(90) van Meer, R.; Gritsenko, O. V.; Baerends, E. J. Physical Meaning of Virtual Kohn−Sham Orbitals and Orbital Energies: An Ideal Basis for the Description of Molecular Excitations. *J. Chem. Theory Comput.* **2014**, *10*, 4432−4441.

(91) Höfener, S.; Gomes, A. S. P.; Visscher, L. Molecular properties via a subsystem density functional theory formulation: A common framework for electronic embedding. *J. Chem. Phys.* **2012**, *136*, 044104.

DOI: 10.1021/acs.jctc.5b00845
J. Chem. Theory Comput. 2015, 11, 5305−5315